

Contents lists available at ScienceDirect

Energy

journal homepage: www.elsevier.com/locate/energy



Efficient production of aromatics by catalytic pyrolysis of fruit waste over zeolites with 3D pore topologies



Yao He ^a, Junjie Chen ^a, Didi Li ^a, Qian Zhang ^b, Dongxia Liu ^c, Jingyong Liu ^a, Xiaoqian Ma ^d, Tiejun Wang ^{b, *}

- ^a Guangdong Key Laboratory of Environmental Catalysis and Health Risk Control, School of Environmental Science and Engineering, Institute of Environmental Health and Pollution Control, Guangdong University of Technology, Guangzhou, 510006, China
- ^b School of Chemical Engineering and Light Industry, Guangdong University of Technology, Guangzhou, 510006, China
- ^c Department of Chemical and Biomolecular Engineering, University of Maryland, College Park, MD, 20742, USA
- ^d Guangdong Key Laboratory of Efficient and Clean Energy Utilization, South China University of Technology, Guangzhou, 510640, China

ARTICLE INFO

Article history: Received 8 June 2020 Received in revised form 27 January 2021 Accepted 1 February 2021 Available online 6 February 2021

Keywords:
Catalytic pyrolysis
Fruit waste
Zeolite
Pore topology
Aromatic compound

ABSTRACT

Fruit waste collected from a juice factory was pyrolyzed over zeolite catalysts with different pore topologies. The production of aromatic compounds was directly influenced by zeolite topology type (i.e. pore opening size and pore channel dimensionality). Zeolites with three-dimensional (3D) pore topologies (e.g. MFI, BEA and FAU) favored aromatization reactions, which yielded up to 80% aromatic compounds, compared to <20% yield in the pyrolysis over FER and MOR zeolites with two- and one-dimensional pore channels, respectively. The catalytic performance of the 3D zeolites, MFI, BEA and FAU were more vulnerable to operating conditions such as catalyst to biomass ratio and pyrolysis temperature, compared to 2D FER and 1D MOR zeolites. The results were possibly explained by the interplays of diffusion limitations and space constrains, imposed by the pore topologies. By correlation analysis, applying FAU zeolite at catalyst to biomass ratio of 2:1 under 450, 550, or 650 °C was found to be optimal for aromatics formation, affording more mono aromatic hydrocarbons (45%) and less polycyclic aromatic hydrocarbons (30%). Moreover, the zeolites employed in the reactions with larger pore size tended to coke. This work potentially provides a guideline for efficient conversion of fruit waste to aromatic compounds enriched biofuels.

© 2021 Elsevier Ltd. All rights reserved.

1. Introduction

The arising concerns of energy security and environment pollution triggered by the overuse of conventional fossil fuels have brought about a formidable challenge to the global industrials [1]. Hence, the publics have been shifting their attention towards the development and deployment of renewable and cleaner resources in the past decades [2]. In this context, biomass that bears a bevy of outstanding merits such as widespreading, easy to obtain, and carbon neutral, becomes to be an optimal candidate for supplementing or substituting traditional resources for the applications in industrial and routine practices [3,4]. In Guangdong Province, China, fruit production is one of the most developed biomass activities. The produced fruits are exported, consumed locally, or

processed into value-added products such as juice and canned fruit. However, fruits are wasted throughout the supply chain, from initial agricultural production down to final household consumption, especially in the industrial processing progress. According to the statistics from Food and Agriculture Organization of the United Nations, nearly half of fruits turns into fruit waste globally each year [5]. This waste is generated in the form of skins, pips and stalks, disposed typically to landfill adding to the burden already placed on these sites [6]. As a category of biomass, the untapped potential of fruit waste is of great economic and environmental significance, considering a global move towards more sustainable development strategies.

Pyrolysis is a disposal technique employing elevated temperature under inert gas atmosphere, capable of converting biomass solids into bio-oil, which is the condensable fraction of pyrolysis vapors. However, as well known this liquid contains a variety of chemical species, resulting in its poor stability and the costly post-processing [7]. Employing catalysts in a pyrolysis process of

^{*} Corresponding author.

E-mail address: tjwang@gdut.edu.cn (T. Wang).

biomass can provide a bio-oil with improved quality, upon catalytically upgrading the primary pyrolysis vapors prior to condensation, which has been assumed to be the concept of catalytic pyrolysis. Catalytic pyrolysis is a one-step process with high flexibility in biomass input, affording a promising pathway to renewables. So far, this technique has been widely employed for handling a variety of biomass feedstocks [8]. Nonetheless, there are few studies covering the topics in catalytic pyrolysis of fruit waste. Park's group earlier performed several investigations including mandarin residue [9] and citrus unshiu peel [10,11]. More recently, some studies associated with citrus waste [12], banana peel [13], and pineapple crown leaves [14] were found.

Catalytic pyrolysis of biomass using zeolite catalysts represents a simple, scalable route to produce valuable chemicals and biofuels, such as aromatic hydrocarbons, which is extremely desired for industry. The zeolitic system renders the advantages of being regenerable and stable over a wide temperature range [15]. Zeolites are crystalline microporous aluminosilicates, equipped with channels and pockets in sizes typically less than 1 nm. Their ordered structure allows them to have shape selectivity towards guest molecules, as a result showing a superb catalytic performance in biomass pyrolysis. To date, zeolites have been widely employed for catalytic pyrolysis of biomass for producing upgraded bio-oils. The studies include a variety of biomass, e.g. cellulose [16], paper industry byproducts [17,18], agricultural wastes [19,20], food waste [21], etc., where the results showed that zeolite topologies play key roles in the catalytic pyrolysis processes, given their interesting properties, particularly for the conversion efficiency (yield of major products). A brief comparison of these processes was made in Table 1. For example, the use of zeolites with SAPO topology in cellulose pyrolysis was able to provide a high yield of furan compounds, e.g. methyl furans and furfural [16]. The authors claimed that the secondary reactions of the furans derived from cellulose decomposition were suppressed by the small size of pore openings in the zeolites. Heeres et al. [17] performed the experiments of black liquor pyrolysis over a range of zeolites and found that medium-pore H-ZSM-5 zeolite resulted in the highest yield of aromatic hydrocarbons. Similar findings were also reported in the catalytic pyrolysis of tea residual [20] and food waste [21]. Besides, a series of large-pore zeolites have also been tested in catalytic pyrolysis. Luo et al. [18] observed that the total yield of aromatic hydrocarbons in lignin pyrolysis over BEA zeolite was comparable with that over H-ZSM-5 zeolite. H-Y zeolite with FAU topology was used for catalyzing the pyrolysis of sugarcane bagasse with high density polyethylene in a fixed-bed reactor by Hassan et al. [19] and they confirmed the effectiveness of the zeolite for upgrading condensable vapors.

Although there are many studies on catalytic pyrolysis of biomass over zeolite catalysts, the applications of this technology for fruit waste disposal are rarely documented, where the influences of topological structures of zeolite on the formation of aromatics are not well understood. In this study, catalytic pyrolysis was applied for the disposal of fruit waste over five commercial zeolites with different topologies. These zeolites have FAU, BEA, MOR, MFI and FER framework structures. It should be noted that BEA and FAU are the representatives for the zeolites with large pore openings and three-dimensional (3D) pore channels, MOR for the large-pore zeolites with one-dimensional (1D) pore channels, MFI for the medium-pore zeolites with 3D pore channels, and FER for the medium-pore zeolites with 2D pore channels. Chemical composition of the products from catalytic pyrolysis of fruit waste over these five zeolite catalysts were examined. Pyrolysis conditions, including catalyst to biomass ratio and reaction temperature, which affected the aromatization effectiveness of the zeolites, were evaluated. Then, analyses were performed for understanding the relationship between desirable mono aromatic hydrocarbons (MAHs) and unwanted polycyclic aromatic hydrocarbons (PAHs) under different scenarios, acquiring the optimal reaction parameters for MAHs formation.

2. Experimental

2.1. Feedstock and catalyst

Fruit waste feedstock is the mixture of juicing residues collected from a juice factory in Guangdong Province, China, which includes a few kinds of fruit such as orange, pineapple, banana, strawberry, grape, etc. It was dried in oven at 105 °C for 24 h and pulverized into powder, and then sieved to pass 80 mesh. Proximate analysis of the feedstock was carried out in accordance to the method of American Society for Testing and Materials (ASTM) D1762-84, affording the information about the content of ash, volatile matter (VM), and fixed carbon (FC) in the sample. Ultimate analysis for the percentage of carbon, hydrogen, nitrogen and oxygen was performed by an elemental analyzer (Vario EL cube, Elementar). In addition, the proportion of hemicellulose and cellulose components of fruit waste was determined according to ASTM D5896-96, and the quantity of lignin was determined by ASTM D1106. The results of these analyses on the fruit waste have been listed in Table 2.

Commercial ammonium form zeolites Ferrierite with FER structure, ZSM-5 with MFI structure, Beta polymorph A with BEA structure, Mordenite with MOR structure, and Faujasite with FAU structure were purchased from Alfa Aesar, and their SiO₂/Al₂O₃ ratios are around 20, which are 20, 23, 25, 20, and 12, respectively. The zeolites were treated in dry air at 550 °C for 4 h to remove organic species adsorbed upon contact with ambient air and to convert ammonium cations to protons. Temperature programmed desorption of ammonia (NH₃-TPD) measurement for the zeolite catalysts was carried out on an auto-catalytic adsorption/desorption system (TP-5080 Xianquan, China) coupled with an online

Table 1 Comparison of catalytic pyrolysis processes.

Feedstock Catalyst		Reactor	Reaction conditions	CFR ^a	Conv. Efficiency ^b	Ref.	
Cellulose	ZrCu/SAPO	Pyroprobe	600 °C, 15 s	8	65.86 area% furans	[16]	
Cellulose	AlCu/SAPO	Pyroprobe	600 °C, 15 s	8	56.94 area% furans	[16]	
Black liquor	H-ZSM-5	μ-Reactor	600 °C, 20 °C/s	20	2.80 wt% benzenes	[17]	
Alkali lignin	H-ZSM-5	Pyrorobe	600 °C, 30 s	5	7.63 wt% aromatics	[18]	
Alkali lignin	H-Y	Pyrorobe	600 °C, 30 s	5	0.77 wt% aromatics	[18]	
Alkali lignin	Н-β	Pyrorobe	600 °C, 30 s	5	2.10 wt% aromatics	[18]	
Bagasse	FAU	Fixed-bed	500 °C, 45 min, 10 °C/min	1/6	55 area% aromatics	[19]	
Tea residual	HZSM-5	Pyroprobe	550 °C, 20 s	1	28.45 C% aromatics	[20]	
Food waste	H-ZSM-5	Pyroprobe	550 °C, 20 s	1	36.40 area% aromatics	[21]	

 $^{^{\}rm a}\,$ CFR = catalyst to feedstock ratio.

^b Conversion efficiency is about the yielding percentage of major product.

Table 2Characterization of fruit waste

Proximate analysis (wt.%) ^a		Ultimate a	Ultimate analysis (wt.%) ^a				Component a	Component analysis (wt.%) ^a		
Ash	VM	FC ^b	C	H	N	S	O ^b	Cellulose	Hemicellulose	Lignin
3.28	81.23	15.49	43.40	5.60	0.79	1.04	49.17	31.40	30.67	13.83

a Dry basis.

thermal conductivity detector (TCD). Prior to the measurement, 100 mg of sample was pretreated under He atmosphere at 500 °C (10 °C/min from room temperature) for 1 h, and then cooled to 100 °C. A flow of 5 vol% NH $_3$ /H $_2$ mixed gas flow was introduced at a flow rate of 30 mL/min for 1 h at 100 °C, followed by He purging for 1 h until a constant signal level was attained in the TCD. Thereafter, the sample was programed heated at a ramping rate of 10 °C/min to 700 °C, and the amount of NH $_3$ in the effluent was measured by the TCD and recorded every 0.1 s.

2.2. Catalytic pyrolysis

The zeolite catalysts and fruit waste biomass were pre-mixed at different weight ratios. In each experiment, the amount of biomass was fixed at 2 mg, and the catalyst loading changed with different catalyst to biomass mixing ratios. A typical experiment was conducted in a semi-batch pyroprobe reactor (Pyroprobe 5200, CDS Analytical) under N₂ atmosphere, which was directly connected to a gas chromatography-mass spectrometry (GC-MS) (Agilent 7890 B-5977A) for analyzing the volatiles evolved from the reactions. The mixture of fruit waste and zeolite catalyst was packed into a 2 mm thick, 20 mm long quartz tube, which was fixed by quartz wool plugging at the both ends, and the tube was then loaded into the pyroprobe reactor for experiments. The pyrolysis experiments were carried out at the temperatures ranging from 450 to 650 °C, with a heating rate of 20 °C/ms for 100 s. Then the pyrolysis vapors were transferred to the GC-MS by He flow through the connection tube where 300 °C was maintained to prevent the vapors from condensation. Meanwhile, the temperature of GC injector was also set to be 300 °C with the split ratio of 1: 100. An Agilent HP-5ms capillary column (30 m \times 0.25 mm \times 0.25 μ m) was employed for chromatographic separation, under a temperature program that was from 50 °C (2 min holding) to 300 °C at a heating rate of 10 °C/min, and held at 300 °C for 5 min. The temperature of the ion source and the scan range of the mass detector were set as 230 °C and 30–300 m/z. The composition of pyrolysis vapor was identified according to NIST library, Wiley library and literatures, and the peak area percentages for each product were recorded for analysis. Although these values are not able to provide the absolute yields of chemical compounds, semi-quantitative evaluation concerning the change in their content can be performed by comparing the values between different scenarios [22,23]. Each experiment was repeated for 3 times and the results were within the error range of $\pm 2\%$.

3. Result and discussion

3.1. Properties of zeolite catalysts

The topological properties of pore networks of zeolites tested in fruit waste pyrolysis are summarized in Table 3. Zeolites are categorized into large-, medium- and small-pore zeolites, according to the size of their pore openings that are typically measured in membered rings (MRs). Amongst the five zeolites in present study, FER and MFI belong to the medium-pore zeolites, while BEA, MOR and FAU are members of the group of large-pore zeolites. The

Table 3Topological characteristics of zeolite catalysts.

Zeolite	Pore topology							
	Shape	Size (nm)	Dimensionality	Graphical representation				
FER	8-MR 10-MR	0.35 × 0.48 0.42 × 0.54	2D	10 MR (0.54 x 0.42 nm) 				
MFI		$0.51 \times 0.55 \\ 0.53 \times 0.56$	3D	10-MR (0.56 x 0.53 nm) 10-MR (0.55 x 0.51 nm)				
BEA	12-MR 12-MR	$0.56 \times 0.56 \\ 0.66 \times 0.67$	3D	12-MR (0.56 × 0.56 nm) 12-MR (0.66 × 0.67 nm)				
MOR	8-MR 12-MR	$0.34 \times 0.48 \\ 0.65 \times 0.70$	1D	12-MR (0.65 x 0.70 nm) 8-MR (0.34 x 0.48nm)				
FAU	12-MR 12-MR	$0.74 \times 0.74 \\ 0.74 \times 0.74$	3D	12-MR (0.74 x 0.74 nm) Supercage (1.3 nm)				

zeolite that has the smallest pore size is FER zeolite, consisting of 2D, perpendicularly intersecting 8-MR (0.48×0.35 nm) and 10-MR $(0.54 \times 0.42 \text{ nm})$ pore channels. MFI zeolite contains two interconnected 10-MR channel systems which run perpendicularly to each other, i.e. straight 10-MR channels (0.56×0.53 nm) in parallel to b-axis and sinusoidal 10-MR channels (0.55 \times 0.51 nm) along the a-axis, which is a 3D medium-pore zeolite that has been widely applied in catalytic pyrolysis [3]. BEA zeolite is the first synthetic large-pore zeolite with 3D intersecting straight channel system of 12-MR [24]. Its straight channels with 12-MR (0.66×0.67 nm) pore size run in two directions along a- and b-axes, respectively, which are cross-linked by zigzag 12-MR channels (0.56 \times 0.56 nm) along c-axis. The framework of MOR zeolite is made up of 12-MR $(0.70 \times 0.65 \text{ nm})$ channels and 8-MR $(0.48 \times 0.34 \text{ nm})$ channels, both of which are straight and extend in the same direction (1D), connected via 8-MR (0.26×0.57 nm) side pockets (not shown in the graphical representation). FAU zeolite owns the largest pore openings in this study which are 12-MR of 0.74×0.74 nm and these large pores are three-dimensionally connected with internal supercages (~1.3 nm). In view of the above analysis, it is found that the pore networks of MFI, BEA and FAU are 3D, while those of FER and MOR are in lower dimensions.

The acidity properties of the samples were measured by the thermal desorption of chemisorbed NH₃. This technique provides general information about the number and distribution of the active acid sites. Two NH₃ desorption peaks were detected in the temperature range of 150–400 °C and >400 °C, which inferred that two sets of acid sites exist on the surface of these zeolite catalysts [25]. The results from NH₃-TPD analysis was summarized in Table 4, where the total amount of desorbed NH₃ enables us to evaluate the concentration of the accessible acid sites. As expected, the acidity

^b Calculated by difference.

Table 4Surface area and acidity characteristics of zeolites

Zeolite	SiO ₂ /Al ₂ O ₃ ^a	Surface area (m ² /g) ^a	Acidity (mmol/g NH ₃) ^b		
			Total	Weak	Mid-strong
FER	20	400	1.14	0.65	0.49
MFI	23	425	1.05	0.57	0.48
MOR	20	500	0.99	0.52	0.47
BEA	25	680	1.32	0.69	0.63
FAU	12	730	0.77	0.33	0.44

^a From manufacture's specification.

and acid strength of the catalysts are close whereby we can further our study on the topological effects of these zeolites.

3.2. Effect of zeolite topology on product composition

3.2.1. Main chemical compositions

The chemical composition of the products of fruit waste pyrolysis over zeolites with different topologies are shown in Table 5. Compounds with the same functional group or with similar property are categorized into one species. For example, anhydro-sugars and anhydro sugar-alcohols makes up the category of sugars, and the miscellaneous oxygenates (mis-oxy) includes ketones, aldehydes and acids, while others involve nitrogen containing molecules such as pyrrole and unidentified chemical compounds. The data in this section was acquired from the pyrolysis reactions under 550 °C at the catalyst to biomass mass ratio of 1 : 1.

Sugars, the main product from primary decomposition, is at a relative yield of 38.74% in non-catalytic circumstance (NC). The FER zeolite catalyst appears to have marginal influences on sugars yield. While less content of sugars is found in the use of MOR, MFI and FAU zeolite, and sugars disappear by using BEA zeolite. The quantities of oxygenates containing cyclopentanones and carboxylic acids are at the same level for FER, BEA and FAU zeolite catalysts as compared to the results of pyrolysis without catalyst. By contrast, MOR zeolite gives the highest yield of mis-oxy, and MFI zeolite is found to yield the least. Similar trend is observed in the variation of furanic compounds. These observations are consistent with the results found in the catalytic pyrolysis experiments of other biomass feedstocks [26]. Phenolics are oxygenated aromatic compounds. Although the addition of zeolite catalysts generally increases their content compared to non-catalytic case, the yield of phenolic compounds is not significant in this work, maintaining at the level lower than 12%. These low yields are opposed to the results of our previous studies where phenols accounted for up to 40% [27]. Since phenolic compounds are mainly derived from lignin during pyrolysis [28], the difference of lignin fractions in biomass feedstocks can cause variations in the yield of phenolic products. The lignin component of the tested fruit waste in current study is around 15 wt% as shown in Table 2, much less than the sawdust

Table 5Chemical species in products of fruit waste pyrolysis over different zeolites.

	Sugars	Mis-oxy ^a	Furans	Phenolics	MAHsa	PAHs ^a	Others
NCa	38.74	13.20	37.28	6.01	_	_	4.77
FER	36.68	14.02	34.98	9.11	2.96	_	2.25
MFI	2.92	5.93	16.62	8.86	29.83	35.84	_
BEA	_	14.24	29.06	7.91	16.42	29.93	2.43
MOR	10.45	20.11	42.45	11.48	6.15	3.89	5.47
FAU	1.84	13.76	29.14	11.73	19.84	20.88	2.80

^a NC, MAHs, PAHs and Mis-oxy are the abbreviations of non-catalytic, mono aromatic hydrocarbons, polycyclic aromatic hydrocarbons, and miscellaneous oxygenates that involves ketones, aldehydes, and acids.

pyrolyzed previously, as a result may leading to the fewer phenolics produced here. Aromatic hydrocarbons are highly valuable products by employing acidic zeolites for catalytic pyrolysis of biomass [29]. They comprise two sub-groups as categorized in this study, that is, MAHs and PAHs. The absence of catalyst in the progress of pyrolysis leads to a lack of aromatic hydrocarbons in condensable vapors. However, adding zeolite can change this situation. The pyrolysis experiments over FER and MOR zeolite catalysts yield a small amount of aromatic hydrocarbons. While the addition of the other zeolites increases the content of aromatics significantly, where the highest amount of aromatic hydrocarbons is obtained by the experiment over MFI zeolite catalyst, giving rise to 29.83% of MAHs and 35.84% of PAHs, followed by BEA and FAU zeolites. This is in accordance to the studies by Lin et al. [30] who examined the catalytic performance of protonated zeolites with MFI, BEA and FAU framework in the pyrolysis of wood-plastic composite, and found that the aromatic hydrocarbons yield was in the order of MFI > BEA > FAU. It is noteworthy that in comparison with FAU zeolite catalysis from which the yield of MAHs and PAHs are of equivalent amount (20%), the PAHs content produced over BEA zeolites occupies higher proportion (30%) with respect to 16.42% MAHs.

3.2.2. Detailed composition of furans and aromatic compounds

In catalytic pyrolysis, furans, along with aromatic compounds that typically contains phenols, MAHs, and PAHs, are valued compounds in great market demand [31]. Fig. 1 presents the distribution of individual compounds in these chemical species, as shown in Fig. 1a-d for furans, phenols, MAHs and PAHs, respectively. Furanic species varies a lot in its composition, and it typically 5-hydroxymethylfurfural furfural, (5-HMF), dimethylfuran (2,5-DMF), isosorbide, and some benzofurans. In the non-catalytic case, 5-HMF is the prevalent compound. While the addition of catalysts mitigates its formation and enhances furfural yield. The amount of 5-HMF is in the order of $NC \approx FER > MOR \approx MFI$, and none can be seen from the experiments by applying BEA and FAU zeolite catalysts. Alternatively, the highest furfural yield is observed in the circumstance of using MOR zeolite. and the yields follows the order $MOR > FAU \approx BEA \approx FER > MFI \approx NC$. In the pyrolysis without catalysts, the results from density functional theory (DFT) calculations showed that the pathways for 5-HMF formation from glucose were preferred over those for furfural [32]. The phenomena observed here suggest that this preference is likely to be altered by the addition of zeolite catalysts, and the altering is most obvious for the reactions using large-pore 3D zeolites as catalysts. Besides, it should be noted that up to 10% of isosorbide and 5% of 2,5-DMF emerge in most scenarios, which are assumed to be of great interest to industry [33,34]. Meanwhile, undesired benzofuran compounds are found in the cases of using the zeolites that are more adept at deoxygenating, which can be associated with the occurrence of condensation reactions between furan molecules on the external surface of these zeolites, indicating an increased tendency towards coking [35].

Phenolic compounds basically include phenol monomer, methylated phenols, and oxygenated phenols, e.g. phenols that contain more than one phenolic hydroxyl groups or have methoxyl groups. The application of large-pore zeolites can double the content of mono phenol, but it generally yields at low levels (<5%), which is due to the small fraction of lignin component in the fruit waste feedstock as shown in Table 2. The trend of phenol yield over different zeolites potentially reveals the influence of pore size. It is likely that larger pore openings facilitate the conversion of large phenolic molecules such as guaiacol into phenol, because of the increased accessibility of the active sites near pore mouth regions.

b Measured by NH₃-TPD.

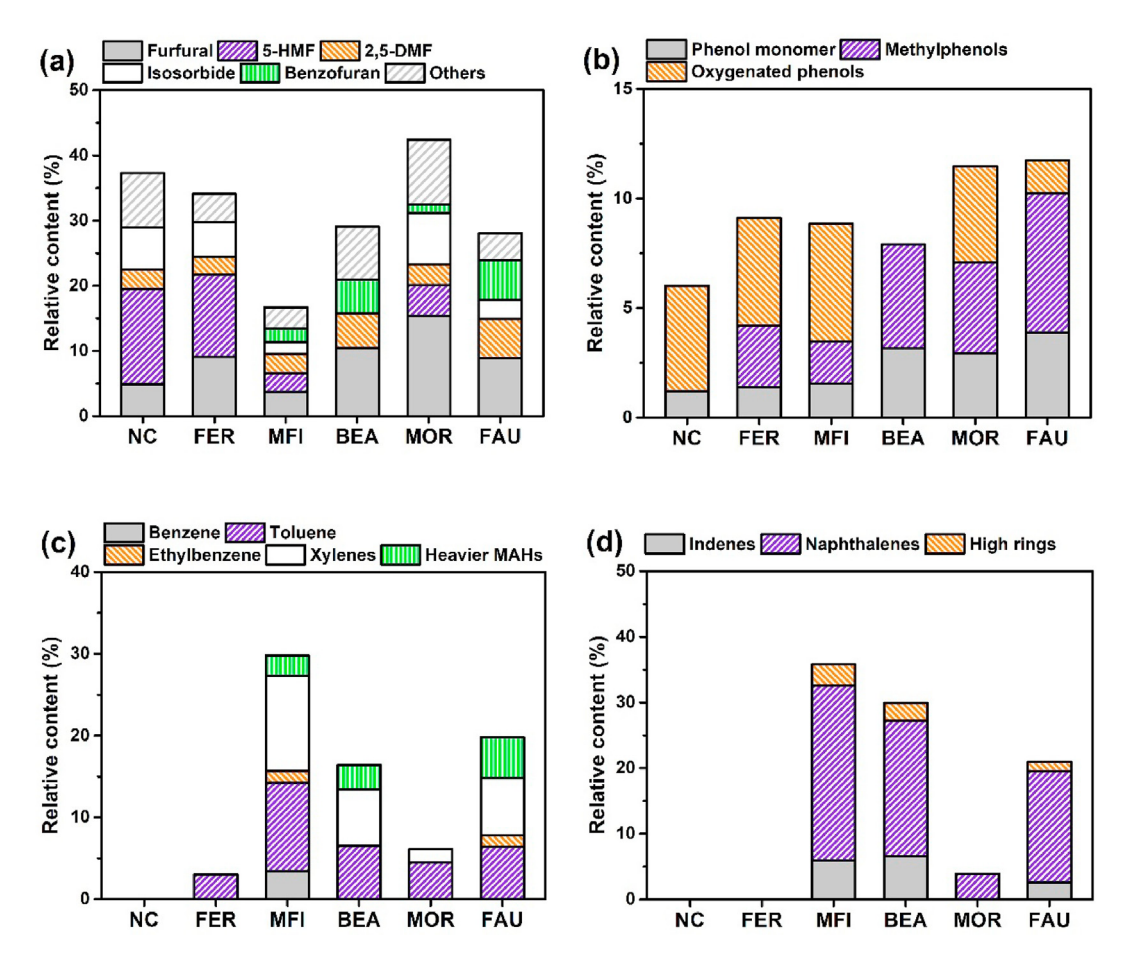


Fig. 1. Constituents of furans (a), phenolics (b), mono aromatic hydrocarbons (c), and polycyclic aromatic hydrocarbons (d) in pyrolysis products with different zeolites.

Previous studies that carried out in aqueous phase have confirmed this potential [36], which is further consolidated by the increased content of methylphenols with the increase in the maximum size of pore openings (FAU > MOR > BEA > MFI > FER), as shown by the violet columns in Fig. 1b. Since methylphenols compounds are mainly derived from transalkylation progress of large alkoxy phenol molecules, and protons afforded by the active sites are essentially required in this process [37].

MAHs species consists of benzene, toluene, ethylbenzene, xylenes (BTEX) and heavier fractions. The species with less molecular weight that contains six to eight carbons (C_6-C_8), i.e. BTEX, are well suited to industrial needs. Methylated benzenes such as toluene and xylenes are found to be commonly existed in the pyrolysis vapors, while benzene can be only found in the catalysis over MFI zeolite. This is consistent with the results of the catalytic conversion of m-cresol to aromatics, where reactions over MFI zeolite gave rise to a higher selectivity to benzene [38]. As claimed by Cheng and Huber [35], the formation of toluene through the reactions between furan and propylene are thermodynamically favorable, which might partially explain the reason for the common existence of this aromatic hydrocarbon. On the other hand, the topological characteristics of zeolites can be also responsible for this phenomenon. Alkylation reactions of benzene molecule are possibly suppressed, to certain extent, by the modest space confinements imposed by the 3D 10-MR pore channels of MFI zeolites [39]. Wider channels may less constrain the occurrence of alkylation, and as a result the already formed benzene is difficult to diffuse out and undergoes further reactions.

In addition, the composition of the undesired fraction in

aromatic hydrocarbons, i.e. PAHs, are shown in Fig. 1d, which is mainly predominated by naphthalene compounds. The change of their total amount is in line with the trend we found in MAHs. This may be because a major route of the PAHs formation is from the conversion of the already formed MAHs [40]. For example, it has been generally proposed that the simplest PAH indene, as shown by the light gray column in Fig. 1d, containing both a five and six membered rings, is formed upon the reactions of benzyl radical with acetylene via hydrogen abstraction and/or acetylene addition [41]. At the same time, multi-ring PAHs such as three fused-ring phenanthrene are found in the cases of employing MFI, BEA and FAU zeolite catalysts. Moreover, it should be mentioned that the PAHs with more fused rings, e. g. chrysene, pyrene, etc. Come out in the products of the catalytic pyrolysis over BEA and FAU zeolites. Both of the zeolites have 3D pore channels of 12-MR, and therefore they would impose less steric constraints which may consequently allow the growing up of the light PAH compounds. Previous studies have confirmed that due to the difference in steric constraints, the catalytic conversion of m-cresols over FAU zeolite formed more heavy PAHs, while the reactions on MFI zeolite mostly produced two aromatic rings with connected alkyl chains [38].

3.2.3. Ternary diagram analysis

The products from fruit waste pyrolysis have been classified into seven species in Table 5, according to their individual functional groups. Therein furans and aromatic compounds that involves oxygenated aromatics (phenolics) and aromatic hydrocarbons are of greater value [31]. For this reason, the composition of products from pyrolysis over different zeolites were analyzed by a ternary

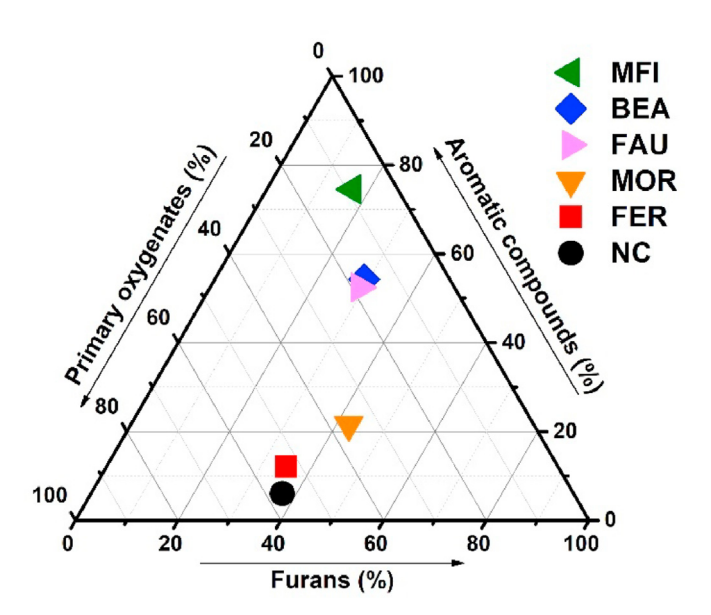


Fig. 2. Ternary diagram for composition of products from pyrolysis over different zeolites

diagram shown in Fig. 2 to evaluate the catalytic effects of the zeolites, concerning furans, aromatic compounds, and the rest chemical species that mainly contains oxygenous compounds commonly existing in primary pyrolysis vapors, e.g. anhydrosugars, ketones, aldehydes, acids, etc., denoted as primary oxygenates. It is clearly that the addition of the zeolite catalysts is able to change the composition of pyrolysis products, resulting in the increase in the content of furans and aromatic compounds and declined yields of primary oxygenates. This suggests the promoting effect of these zeolites on deoxygenation reactions, which agrees with the nature of Brønsted acids in biomass catalysis [42]. Among the zeolites, FER shows to have the least effect on primary pyrolysis vapors, as the point of FER in Fig. 2 stays quite close to the non-catalytic reference point. While using MOR zeolite can reduce the primary oxygenated compounds to 40% (compared to 60% in the non-catalytic scenario, NC) and enhance furans yielding. Both FER and MOR zeolites, however, are less capable of affording aromatic compounds, giving rise to the yields lower than 20%. It is interesting that although their pore sizes differ from each other, the pore networks of both are not well-developed and neither has 3D pore channels as presented in Table 3. In contrast, the changes in composition incurred by the employment of MFI, BEA, and FAU zeolites are much more significant. By using FAU and BEA zeolites, over 55% yield of aromatic compounds and two thirds reduction of primary oxygenates are achieved. Moreover, with the use of MFI zeolite, the content of aromatic compounds further increases, approximating to 80% accompanied with less than 10% yield of primary oxygenates, which suggests its superior aromatization and deoxygenation ability. The pore openings are of medium size (10 MR) for MFI, and of large size (12 MR) for FAU and BEA, but the pore channels extend in 3D for all of them. These observations hint that in addition to the size of pore openings, the dimensionality of pore channels also closely relates to the reactions of catalysis for deoxygenation and/or aromatization in fruit waste pyrolysis. The influence of pore network dimensionality of zeolite on product distribution was reported previously in the studies of olefin oligomerization [43]. The authors found that zeolites with higher dimensional pore architecture enhanced the yield of multi chain-branched oligomers, while 1D channel systems such as ZSM-22 and ZSM-23 were able to minimized the number of chain branching for oligomerization

products.

3.3. Catalytic performance of zeolites in different pyrolysis conditions

3.3.1. Product distribution

The pyrolysis conditions, i.e. catalyst to biomass ratio (CFR) and pyrolysis temperature, were herein investigated. Since these parameters are closely related to the catalytic performance of zeolites, and will affect the improved economics and commercial deployment of the pyrolysis technology [44]. Fig. 3 shows the influence of the pyrolysis conditions on the catalytic performance of each zeolite catalyst in terms of product distribution. We tested three catalyst loadings that are 1, 2, and 4 mg equal to catalyst to biomass mass ratio of 1:2,1:1, and 2:1. The experiments of these three loadings were carried out at 450, 550, and 650 °C, respectively. As shown in Fig. 3, the horizontal axis represents pyrolysis conditions. The general trend is that furans, sugars and mis-oxy compositions decrease, and the content of aromatic compounds, including phenols and aromatic hydrocarbons, increases with the increase in catalyst to biomass ratio and reaction temperature. It is obvious that the catalyst to biomass ratio plays a leading role and, the influence of the pyrolysis conditions on product distribution are different for different zeolite catalysts.

The catalytic effectiveness is less influenced by the pyrolysis conditions for the zeolites with limited aromatization capability. For the reactions over 2D medium pore FER zeolite catalyst, the tested catalyst loadings and pyrolysis temperatures are of marginal influence on the yield of products. Sugars are in significant amount at all scenarios, and their yield is slightly reduced with increased catalyst loading. Furans produced at 450 °C are above 40%, slightly more than that obtained at 550 and 650 °C. Aromatic hydrocarbons are not detected at 450 °C, and only small amounts can be found in the results at higher temperatures. MOR zeolite catalyst having 1D channel systems but much larger pore size (12-MR), compared to FER, is more sensitive to reaction conditions. For example, sugars are reduced sharply as catalyst loading increases. As comparing the consequences of the highest and the lowest catalyst additions, it can be found that the sugars were reduced by up to three quarters with increased catalyst to biomass ratio.

Alternatively, the pyrolysis conditions greatly influence the catalytic performance of the 3D topology zeolites which are capable of providing a relatively high yield of aromatic compounds. The performance of zeolite with MFI structure, a class of medium-pore zeolite similar to FER but having pore structure developed threedimensionally give rise to a high yield of aromatics in most cases. At CFR = 1: 2,450 °C, the yield of aromatic hydrocarbons (MAHs plus PAHs) reaches to 20%, which is then doubled with increasing pyrolysis temperature. In parallel, at 450 °C as catalyst to biomass ratio increases to CFR = 2: 1, the aromatics yield grows to nearly 90%. For the large-pore, 3D zeolites BEA and FAU, the influences caused by pyrolysis conditions on product distributions are similar, as shown in Fig. 3d and e. The change in catalyst to biomass ratio shows to be fairly influential. It is found that the higher the catalyst to biomass ratio, the easier the formation of aromatics. For example, the contents of aromatic hydrocarbons are <25% for BEA and <15% for FAU at CFR = 1 : 2, and they increase to $\sim80\%$ when R increases to 2:1.

The products in the catalysis using of BEA and FAU zeolites are generally lack of sugar species but abundance of furans, phenols and mis-oxy. Merely 8.69% of sugars can be observed at CFR =1: 2, 450 °C over BEA zeolite catalyst in comparison to 30.78% over MFI zeolite catalyst under the same pyrolysis condition, and the yield further declines to 1.94% as reaction temperature increases to 650 °C. The small amount of sugars formed over BEA and FAU

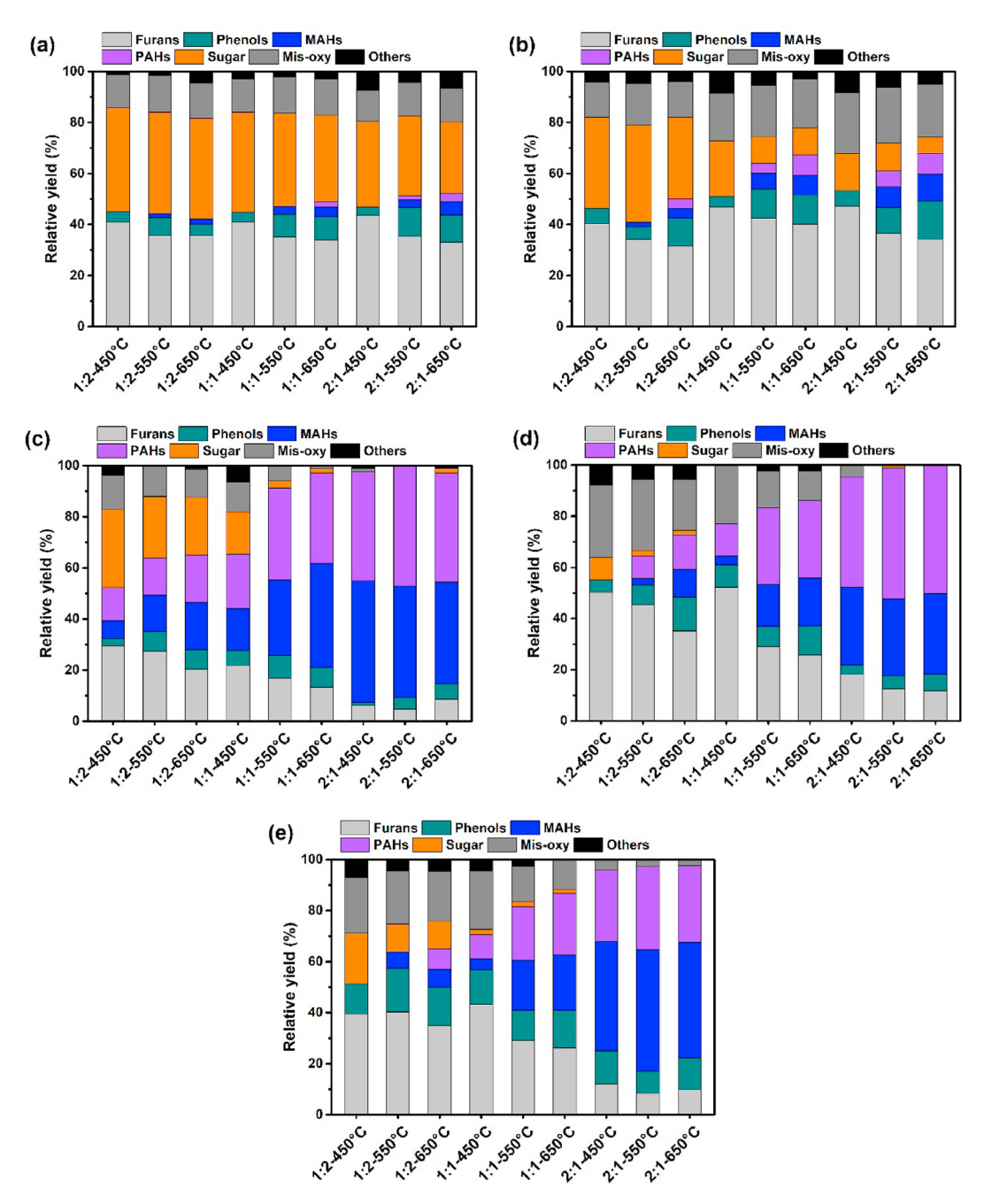


Fig. 3. Product distribution under different pyrolysis conditions over FER (a), MOR (b), MFI (c), BEA (d), and FAU (e) zeolite catalysts.

zeolites may reflect a strong ability of the zeolites for dehydration and/or cracking of primary pyrolysis vapors owing to their large pore openings. This agrees with previous studies where the large-pore zeolite was particularly applied for the cracking of coal tar that contained a range of large molecules [45]. In addition, it is found that the phenols yield is mostly higher in FAU zeolite catalysis, compared to that attained through the use of other zeolite catalysts or without the use of catalyst. The content of phenols achieves 17.26% at CFR = 1:2,550 °C, which is twice more than that over other zeolites under the same condition. This high yield of phenols likely owes to the enhanced cracking behaviors of phenol oligomers derived from the lignin fraction of fruit waste, resulted from the 0.74 \times 0.74 nm apertures and unique supercage structure. In the studies on pyrolysis of lignin over a series of zeolites, FAU

zeolite was the most effective zeolite for phenolic monomers production and the authors also ascribed that to its large pore openings [46].

3.3.2. Ternary diagram analysis

Fig. 4 intuitively compares the influences of pyrolysis conditions on catalytic performance of the tested zeolites with different pore topologies by ternary diagrams, with respect to the content of aromatic compounds, furans and primary oxygenates. The different geometries in green, red and blue colors corresponds to the product compositions of catalytic pyrolysis under different pyrolysis conditions. The black dot that signifies the composition obtained from the experiment performed at 550 °C without catalyst addition stays in the diagrams as a non-catalytic reference point. As can be seen in

Low-dimension zeolite

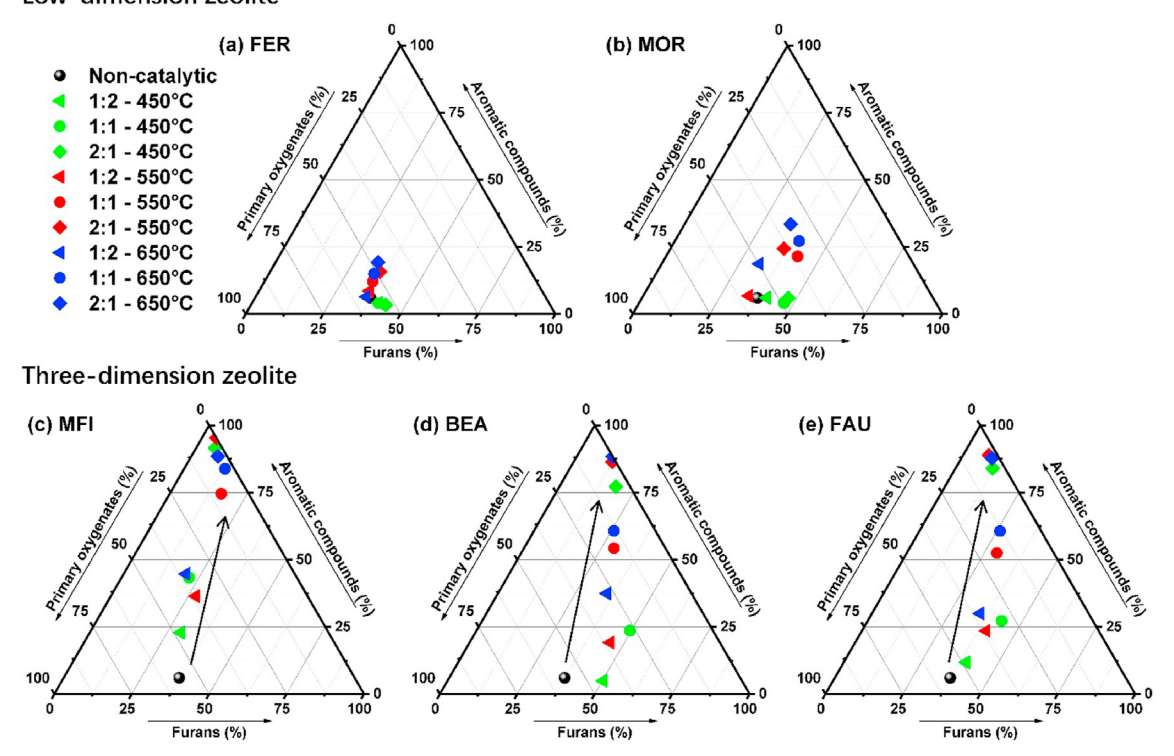


Fig. 4. Influence of pyrolysis conditions on catalytic performance of zeolites FER (a), MOR (b), MFI (c), BEA (d), and FAU (c) using ternary diagrams of primary oxygenates, furans, and aromatic compounds.

Fig. 4a, the colored geometries are distributed fairly close to the black dot, reflecting that the compositions of pyrolysis vapor at all the tested conditions over FER zeolite catalyst are similar to that in the non-catalytic scenario. The change in pyrolysis conditions brings about a minor influence on the catalytic performance of this 2D medium-pore zeolite, which is consistent with what we found in Fig. 3. In contrast, the colored geometries are somewhat scattered with the use of 1D large-pore MOR zeolite. Its use obviously affords more furans at the low temperature and more aromatic compounds at higher temperatures.

By employing the 3D zeolites, the colored points spread out rather than stay around the reference dot, which visually indicates the increased susceptibility of the aromatization effectiveness of the zeolites to pyrolysis conditions. MFI zeolite catalyst owns the greatest capability for aromatization. It can catalyze fruit waste to produce over 75% aromatic compounds under a number of pyrolysis conditions, while the content of furans correspondingly declines. The same trends were observed in pyrolysis of southern yellow pine over H-ZSM-5 zeolite catalyst by Ragauskas' group [47]. They confirmed the increase in aromatic extent of pyrolysis vapors with increasing catalyst addition and/or elevating reaction temperature by using ¹³C nuclear magnetic resonance analysis. By contrast, the catalytic performances of BEA and FAU zeolites are relatively more susceptible, as can be seen from the scattered distributions of the colored geometries in Fig. 4d and e. Their employment typically produced very small amounts of aromatic compounds at low catalyst to biomass ratio (CFR = 1: 2) under low pyrolysis temperature 450 °C, but the yield of aromatic compounds arises sharply as the ratio and/or the temperature increases. High yields of aromatic compounds (>75%) are mainly obtained in the scenarios at CFR = 2:1 catalyst to biomass ratio.

For the formation of aromatic compounds, the catalytic performance of zeolites with low dimensional topologies such as 2D FER

and 1D MOR that are less reactive, can be little affected by pyrolysis conditions. In comparison, the performance of zeolite catalysts with 3D pore channels, i.e. MFI, BEA and FAU zeolite, which can effectively produce aromatic compounds, are more vulnerable to pyrolysis conditions.

3.4. Possible mechanism

Fig. 5 graphically depicts the effects of pore channel dimensionality and pore opening size on aromatics formation in the pyrolysis of fruit waste over different zeolite catalysts. In the progress of the reactions, cellulose and hemicellulose in biomass are initially transformed to form anhydrosugars and small oxygenates by ring scissions, and the sugars then occur dehydration reactions and form furans [42]. These dehydration reactions can occur without catalyst, or at the outer surface or pore mouth region in zeolites, while aromatic compounds are primarily formed upon the aromatization of the furans on the acid sites inside pore channels [35]. Fig. 5 demonstrates the idea about the influence of zeolite topology by taking the furanic molecules as an example, of which the kinetic diameters are larger than 0.5 nm [39]. That is, the dimensionality of pore channels and the size of pore openings both act on the diffusion behavior of furans, which consequently affects the yield of aromatic hydrocarbons.

Over 2D FER zeolite catalysts, furanic compounds derived from anhydrosugars in primary pyrolysis vapor through the catalysis of the active sites on the outer surface of the zeolites, may not diffuse into the channels of FER zeolite and access the internal active sites due to the smaller size of the pore openings (8-MR) which is around 0.4 nm in diameter (<0.5 nm of furan molecules). Therefore, furans once form, they can be hardly consumed and converted into aromatics over FER zeolite catalyst, which results in a high yield of furans (35%). Nevertheless, different circumstance occurs in the

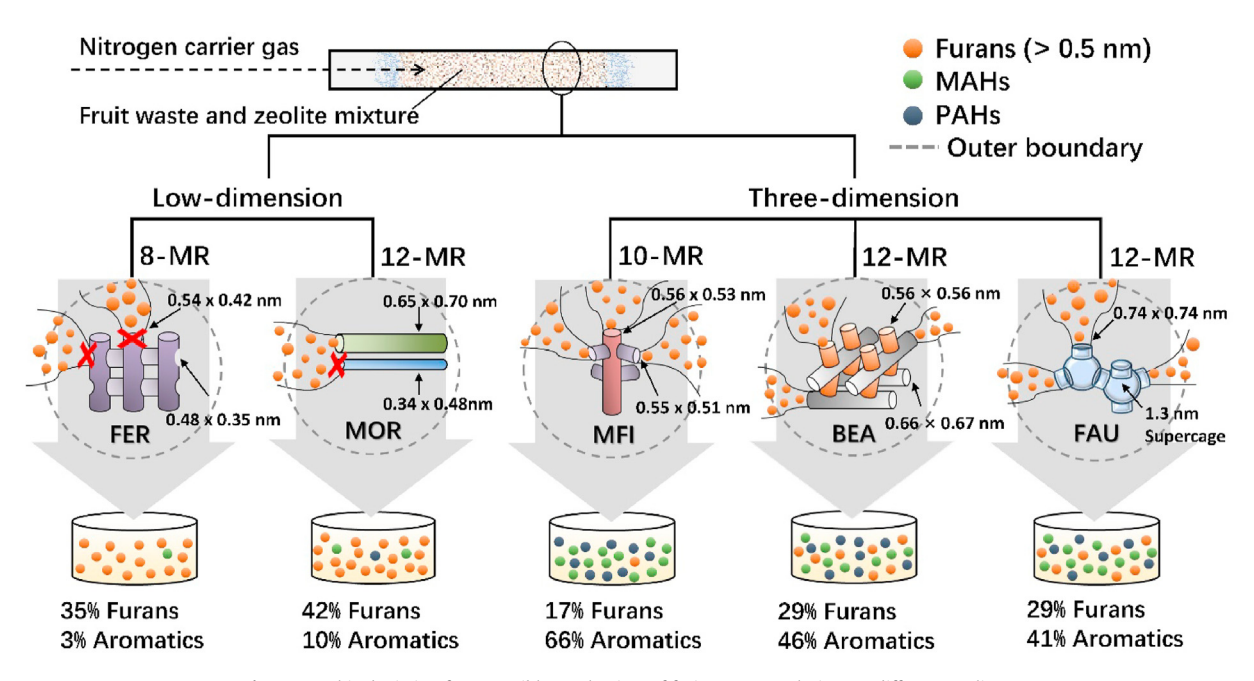


Fig. 5. Graphic depiction for a possible mechanism of fruit waste pyrolysis over different zeolites.

reactions using MOR zeolite catalyst equipped with 1D channels. Although the as-formed furans cannot enter the smaller 8-MR pores in MOR zeolite, of which the size is 0.34×0.48 nm, they are able to diffuse into the zeolite's 12-MR pore channels. Unfortunately, during internal diffusion progress, the furan molecules may have less chance to bond with the active sites along their transfer route and undergo aromatization reactions due to the mono-dimensional pore structures of MOR zeolite. This is supported by the work of Guisnet et al. [48] who claimed that for aromatization, a sufficient number of acid sites has to be present along a path of diffusion. At the same time, around the pore mouth region of the MOR zeolite, the anhydrosugars in primary pyrolysis vapor are likely to be catalyzed for dehydration and form furans. As a result, higher yield of furans is observed in the MOR zeolite catalysis.

In comparison, in the reactions over MFI, BEA and FAU zeolite catalysts that all have 3D pore topologies and larger pore sizes $(\geq 10 \text{ MR})$, furan molecules are allowed to enter the pore channels and thereafter move three dimensionally. This provides the furan molecules greater potential for accessing the active sites embedded on the inner surface of the pore channels. Thus, more furans are converted and transformed into aromatic hydrocarbons over these 3D zeolite catalysts. It is noteworthy that the high yield of aromatic compounds in the pyrolysis over MFI zeolite catalyst should additionally be credited to its moderate steric constraints resulted from the 10-MR pore openings (~0.5 nm in diameter) and the zigzag channel system. However, the 12-MR BEA and FAU zeolite catalysts that similarly have 3D pore topologies where the pore openings are relatively large (~0.6 nm and ~0.7 nm in diameter for BEA and FAU, respectively), may impose less spatial confinement, which can be also a result of different shapes of pore channel systems (straight for BEA zeolite and supercage for FAU zeolite) other than zigzag form in MFI zeolite. This fact mitigates the aromatization reactions and reduces the conversion of the as-formed furans. In other words, the furans are less consumed forming aromatic hydrocarbons over BEA and FAU zeolites compared to MFI zeolite, giving rise to the higher yields of furans and the lower yield of aromatics. These impacts of pore channels have been evidenced in previous studies reported by Iglesia's group for carbonylation of dimethyl ether [49].

They found that the reactions that produces methyl acetate proceeded particularly fast in the catalysis by applying MOR and FER zeolite catalysts, which both have 8-MR pores. By employing larger pore zeolites, the reaction rates were low or undetectable. Similar findings concerning the effects of confined space were also documented by Huang et al. [50] who performed the studies in transalkylation of 4-propylpehnol with benzene and found that, compared to 12-MR MOR and FAU zeolite catalysts, 10-MR MFI zeolite was able to catalyze the transalkylation reactions more effectively owing to its moderate steric constraints.

3.5. Production of MAHs vs. PAHs

Aromatic hydrocarbons are the compounds of highest economic value amongst the chemical species in pyrolysis products, as they are essential building blocks of the chemical industry for the production of a broad range of solvents, polymers, and fine chemicals [29]. Particularly, MAHs such as benzene, toluene, ethylbenzene, and xylenes, are important intermediates for chemical engineering [51], and these aromatic hydrocarbons can be applied directly as drop-in fuel additives [52]. While PAHs are considered to be less valuable. Such large molecular aromatics are assumed as the major precursors responsible for coke formation, which subsequently deactivates the zeolite catalyst in catalytic pyrolysis [53].

On account of these, the relative yield of MAHs against PAHs from pyrolysis of fruit waste under various reaction parameters including the type of zeolite employed were correlatively analyzed. The cases where aromatic compounds are highly prevalent, e.g. more than 50% (refer to Fig. 4), are analyzed, as presented in Fig. 6. It is shown that most of the scenarios over MFI, BEA and FAU zeolite catalysts are involved. We categorized these cases from left to right into three groups. Group I corresponds to the lower yield of both MAHs and PAHs. Larger amount of aromatic hydrocarbons can be found in the cases of group II and III, where group II corresponds to a higher yield of MAHs (~45%) and a lower yield of PAHs (~30%) compared to group III. Since higher content of MAHs with lower levels of PAHs is strongly desired for the production of aromatic hydrocarbons in catalytic pyrolysis, it can be said that the reaction parameters in group II are relatively optimal, which contains the

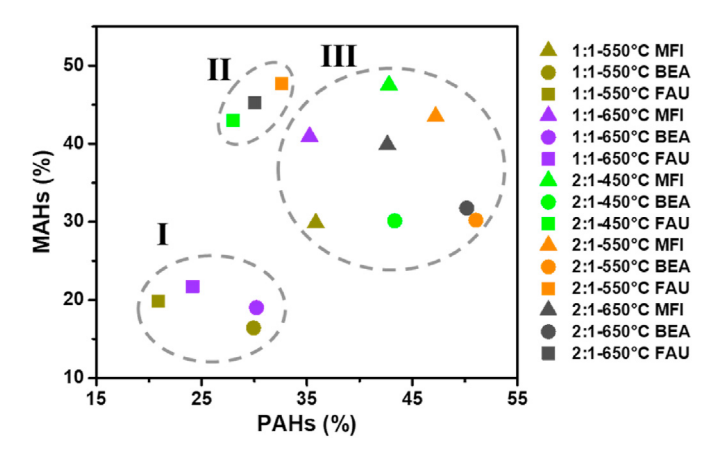


Fig. 6. Evaluation of MAH vs. PAH products from pyrolysis under different reaction parameters.

cases using FAU zeolite catalyst at catalyst to biomass ratio of 2 : 1 under the pyrolysis temperatures of 450, 550, and 650 $^{\circ}$ C.

It is noted that though the pyrolysis reactions over MFI zeolite produce comparable amounts of MAHs in most cases compared to group II, more PAHs are simultaneously formed. Besides, the interesting thing is that BEA zeolite catalyst tends to catalyze the conversion of fruit waste to PAHs, rather than MAHs, at the increased catalyst to biomass ratio (CFR = 2:1), as shown by the circles at the bottom-right in Fig. 6. This is consistent with the findings by Luo et al. [18] who used the catalyst to biomass mass ratio of 5: 1 in lignin pyrolysis and found that less MAHs and more PAHs were attained by using BEA in comparison with MFI and FAU zeolite catalysts. Similar trend was also observed by Ibarra et al. [54] in the experiments of catalytic cracking of raw bio-oil. This is possible in that: for MFI zeolite catalyst, the modest steric constraints imposed by its medium size pore channel could greatly suppress the formation of large aromatic molecules; for FAU zeolite catalyst that consists of large pore openings (0.74 \times 0.74 nm) and supercage structure (1.3 nm in diameter), the formed MAHs can be rapidly released before they have a chance to react further forming heavier products; while the 0.56 \times 0.56 nm and 0.66 \times 0.67 nm pore channels of BEA zeolite are less capable of having both effects. This is supported by the findings from the work of Zheng et al. [40], who argued that there exists a trade-off of diffusion and space confinement for the formation of aromatic hydrocarbons.

3.6. Deposition of coke in different zeolite catalysts

In order to characterize the coke deposition on the five types of zeolite catalyst, feedstock and zeolite were separately placed in the reaction quartz tube and fixed by quartz wool for catalytic pyrolysis experiments. In these experiments, the catalyst to biomass ratio was 2: 1 and the reactions were performed at 650 °C. Then, the spent zeolite catalysts were collected for temperature programmed oxidation (TPO) test by a thermogravimetric analyzer (TGA/DSC1, METTLER TOLEDO) at a heating rate of 10 °C/min from room temperature to 800 °C under 80 mL/min air. Blank tests were conducted to obtain the baseline before the experiments. Each thermogravimetric result was subtracted from the baseline to reduce the buoyancy effects [55]. The TPO curves of the spent catalysts were shown in Fig. 7, where the weight loss rate was plotted against temperature. The weight loss of catalyst is due the combustion of coke deposition, and the temperature region of weight loss indicates the development and/or the location of the coke. The higher the coke content, the more difficult the removal through oxidative treatment. It can be observed that the condensation degree of coke five zeolites complies in the with the order MFI < FER < MOR < BEA < FAU. Analogous phenomena were found previously in the catalytic pyrolysis of wood-plastic composite [30]. The authors claimed that the supercage structure in FAU was conductive to coke formation, while the moderate pore size of MFI hampered the entering of phenols which was regarded as one of the predominating precursors of coke [56]. In other words, the zeolite catalysts that possess large pore channels (12-MR) are prone to coke during catalytic pyrolysis. This was also evidenced by Elordi et al. [57] who cracked high density polyethylene with zeolite catalysts. As the deconvolutions of the TPO curves shown in Fig. 7b, for the used MFI and FER zeolite catalysts, there are two peaks on the TPO curves, in the temperature ranges of 400-500 °C and 500-650 °C, respectively. On the TPO curve of the used MOR, BEA and FAU zeolite catalysts, the peak at lower temperature does not exist, and only one peak can be found above 500 °C. According to previous studies [58], the ones at lower temperatures stem from the oxidation of less developed coke that located on the external surface of the zeolite catalyst, and the ones at higher temperatures are related to the coke that is highly aromatic, formed mainly by dehydrogenation near the active sites on the inner surface of pore channels. Accordingly, the spent MOR zeolite may have the most recalcitrant coke as its TPO peak appears at the highest temperature 585 °C among the tested zeolite catalysts. The TPO peaks above 500 °C for the rest of the spent zeolite catalysts correspond to the

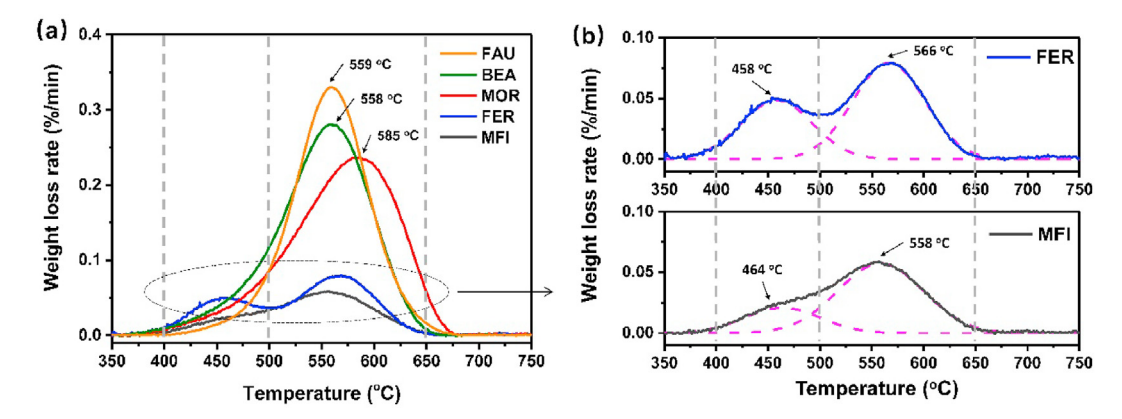


Fig. 7. (a) TPO results of the used zeolite catalysts (b) deconvolution of TPO curves of the used FER and MFI zeolite catalysts (650 °C, catalyst to biomass ratio = 2 : 1).

temperatures from 558 to 566 °C which refers to the burning of the coke with less condensed composition. Besides, Moljord et al. [59] proposed that the ease of coke oxidation was correlated with the distribution of framework aluminum that is affected by zeolite topology. In other words, the difference in structure of zeolite would result in different oxidation behavior of coke, which can be ascribed to the ability of oxygen molecules to access coke in the oxidation process. The higher decomposing temperature of the carbonaceous deposit in MOR zeolite catalyst, therefore, may be additionally related to the restraints of oxygen-coke contact imposed by its mono-dimensional pore topology.

4. Conclusion

Producing aromatics from biomass waste represents a flexible and carbon neutral route for green chemicals and renewable energy. In this study, catalytic pyrolysis of fruit waste was performed over zeolite catalysts with different pore topologies. The catalytic pyrolysis over zeolites with 3D pore channels (i.e. MFI, BEA and FAU) were more effective for aromatization reactions, which affords ~80% aromatic compounds compared to less than 20% of that over 1D FER and 2D MOR zeolites. The catalytic performance of MFI, BEA and FAU zeolites were susceptible to pyrolysis conditions, by which the FER and MOR zeolites were less influenced. These results can be possibly ascribed to the interactive effect of diffusion limitations and space confinements interactions, which are imposed by pore channel dimensionality and pore opening size of the zeolites. Catalytic pyrolysis over FAU zeolite at CFR = 2:1 under 450, 550, and 650 °C allowed more MAHs (45%) and less PAHs (30%) formation, which was considered to be the optimal combination of reaction parameters. Besides, the deposition degree of coke of the spent zeolite catalysts was in the order of MFI < FER < MOR < BEA < FAU. From these, a guideline can be established for producing aromatic compound enriched biofuels through catalytic pyrolysis of fruit waste.

Credit author statement

Yao He: Conceptualization, Methodology, Writing — original draft, Junjie Chen: Investigation, Formal analysis, Didi Li: Data curation, Visualization, Qian Zhang: Formal analysis, Validation, Dongxia Liu: Writing — review & editing, Jingyong Liu: Project administration, Xiaoqian Ma: Funding acquisition, Resources, Tiejun Wang: Supervision, Writing — review & editing.

Declaration of competing interest

The authors declare that they have no known competing financial interests or personal relationships that could have appeared to influence the work reported in this paper.

Acknowledgement

The authors gratefully acknowledge the support from National Natural Science Foundation of China (51806040 and 51978175), 2017 Central Special Fund for Soil "Preliminary Study on Harmless Treatment and Comprehensive Utilization of Tailings in Dabao Mountain" (18HK0108), and the Key Lab of Pollution Control and Ecosystem Restoration in Industry Clusters, Ministry of Education, South China University of Technology. Y. He acknowledges Z. Wang at Jinan University and X. Chen at South China University of Technology.

References

- [1] Chen Y-K, Lin C-H, Wang W-C. The conversion of biomass into renewable jet fuel. vol. 201. Energy: 2020.
- [2] Guan W, Tsang C-W, Lin CSK, Len C, Hu H, Liang C. A review on high catalytic efficiency of solid acid catalysts for lignin valorization. Bioresour Technol 2020:298
- [3] Chen X, Che QF, Li SJ, Liu ZH, Yang HP, Chen YQ, Wang XH, Shao JG, Chen HP. Recent developments in lignocellulosic biomass catalytic fast pyrolysis: strategies for the optimization of bio-oil quality and yield. Fuel Process Technol 2019:196.
- [4] Onarheim K, Hannula I, Solantausta Y. Hydrogen enhanced biofuels for transport via fast pyrolysis of biomass: a conceptual assessment. Energy 2020:199.
- [5] FAO. Global food losses and food waste Extent. Rome: causes and prevention; 2011.
- [6] Deng G-F, Shen C, Xu X-R, Kuang R-D, Guo Y-J, Zeng L-S, Gao L-L, Lin X, Xie J-F, Xia E-Q, Li S, Wu S, Chen F, Ling W-H, Li H-B. Potential of fruit wastes as natural resources of bioactive compounds. Int J Mol Sci 2012;13:8308–23.
- [7] Sharifzadeh M, Sadeqzadeh M, Guo M, Borhani TN, Konda NVSNM, Garcia MC, Wang L, Hallett J, Shah N. The multi-scale challenges of biomass fast pyrolysis and bio-oil upgrading: review of the state of art and future research directions. Prog Energy Combust Sci 2019;71:1–80.
- [8] Gholizadeh M, Hu X, Liu Q. A mini review of the specialties of the bio-oils produced from pyrolysis of 20 different biomasses. Renew Sustain Energy Rev 2019;114:109313.
- [9] Kim JW, Park SH, Jung J, Jeon J-K, Ko CH, Jeong K-E, Park Y-K. Catalytic pyrolysis of Mandarin residue from the Mandarin juice processing industry. Bioresour Technol 2013;136:431–6.
- [10] Kim B-S, Kim Y-M, Jae J, Watanabe C, Kim S, Jung S-C, Kim SC, Park Y-K. Pyrolysis and catalytic upgrading of Citrus unshiu peel. Bioresour Technol 2015;194:312–9.
- [11] Kim Y-M, Jae J, Lee HW, Han TU, Lee H, Park SH, Kim S, Watanabe C, Park Y-K. Ex-situ catalytic pyrolysis of citrus fruit peels over mesoporous MFI and Al-MCM-41. Energy Convers Manag 2016;125:277—89.
- [12] Alvarez J, Hooshdaran B, Cortazar M, Amutio M, Lopez G, Freire FB, Haghshenasfard M, Hosseini SH, Olazar M. Valorization of citrus wastes by fast pyrolysis in a conical spouted bed reactor. Fuel 2018;224:111–20.
- [13] Ozbay N, Yargic AS, Sahin RZY, Yaman E. Valorization of banana peel waste via in-situ catalytic pyrolysis using Al-Modified SBA-15. Renew Energy 2019;140: 633—46
- [14] Barbosa AS, Siqueira LAM, Medeiros RLBA, Melo DMA, Melo MAF, Freitas JCO, Braga RM. Renewable aromatics through catalytic flash pyrolysis of pineapple crown leaves using HZSM-5 synthesized with RHA and diatomite. Waste Manag 2019:88:347–55.
- [15] Bhoi PR, Ouedraogo AS, Soloiu V, Quirino R. Recent advances on catalysts for improving hydrocarbon compounds in bio-oil of biomass catalytic pyrolysis. Renew Sustain Energy Rev 2020;121.
- [16] Chen X, Chen Y, Chen Z, Zhu D, Yan H, Liu P, Li T, Chen H. Catalytic fast pyrolysis of cellulose to produce furan compounds with SAPO type catalysts. J Anal Appl Pyrol 2018;129:53–60.
- [17] Heeres A, Schenk N, Muizebelt I, Blees R, De Waele B, Zeeuw A-J, Meyer N, Carr R, Wilbers E, Heeres HJ. Synthesis of bio-aromatics from black liquors using catalytic pyrolysis. ACS Sustainable Chem Eng 2018;6:3472–80.
- [18] Luo Z, Lu K, Yang Y, Li S, Li G. Catalytic fast pyrolysis of lignin to produce aromatic hydrocarbons: optimal conditions and reaction mechanism. RSC Adv 2019;9:31960–8.
- [19] Hassan H, Lim JK, Hameed BH. Catalytic co-pyrolysis of sugarcane bagasse and waste high-density polyethylene over faujasite-type zeolite. Bioresour Technol 2019;284:406—14.
- [20] Wang J, Zhong Z, Zhang B, Ding K, Xue Z, Deng A, Ruan R. Upgraded bio-oil production via catalytic fast co-pyrolysis of waste cooking oil and tea residual. Waste Manag 2017;60:357–62.
- [21] Zhang B, Zhong Z, Min M, Ding K, Xie Q, Ruan R. Catalytic fast co-pyrolysis of biomass and food waste to produce aromatics: Analytical Py—GC/MS study. Bioresour Technol 2015;189:30—5.
- [22] Lu Q, Guo H-q, Zhou M-x, Zhang Z-x, Cui M-s, Zhang Y-y, Yang Y-p, Zhang L-b. Monocyclic aromatic hydrocarbons production fromcatalytic cracking of pine wood-derived pyrolytic vapors over Ce-Mo2N/HZSM-5 catalyst. Sci Total Environ 2018;634:141–9.
- [23] Chen L, Liao Y, Guo Z, Cao Y, Ma X. Products distribution and generation pathway of cellulose pyrolysis. J Clean Prod 2019;232:1309–20.
- [24] Liu Z, Ohsuna T, Terasaki O, Camblor MA, Diaz-Cabañas M-J, Hiraga K. The first zeolite with three-dimensional intersecting straight-channel system of 12membered rings. J Am Chem Soc 2001;123:5370–1.
- [25] Arena F, Dario R, Parmaliana A. A characterization study of the surface acidity of solid catalysts by temperature programmed methods. Appl Catal Gen 1998;170:127–37.
- [26] Chagas BME, Dorado C, Serapiglia MJ, Mullen CA, Boateng AA, Melo MAF, Ataíde CH. Catalytic pyrolysis-GC/MS of Spirulina: evaluation of a highly proteinaceous biomass source for production of fuels and chemicals. Fuel 2016;179:124–34.
- [27] He Y, Chen S, Chen J, Liu D, Ning X, Liu J, Wang T. Consequence of replacing nitrogen with carbon dioxide as atmosphere on suppressing the formation of

- polycyclic aromatic hydrocarbons in catalytic pyrolysis of sawdust. Bioresour Technol 2020;297:122417.
- [28] Lu Q, Zhang Z-x, Ye X-n, Li K, Cui M-s, Yang Y-p. Catalytic fast pyrolysis of alkali-pretreated bagasse for selective preparation of 4-vinylphenol. J Anal Appl Pyrol 2019;143.
- [29] Genuino HC, Muizebelt I, Heeres A, Schenk NJ, Winkelman JGM, Heeres HJ. An improved catalytic pyrolysis concept for renewable aromatics from biomass involving a recycling strategy for co-produced polycyclic aromatic hydrocarbons. Green Chem 2019;21:3802–6.
- [30] Lin X, Zhang Z, Wang Q. Evaluation of zeolite catalysts on product distribution and synergy during wood-plastic composite catalytic pyrolysis. Energy 2019:189
- [31] Guo T, Li X, Liu X, Guo Y, Wang Y. Catalytic transformation of lignocellulosic biomass into arenes, 5-hydroxymethylfurfural, and furfural. ChemSusChem 2018:11:2758–65.
- [32] Hu B, Lu Q, Jiang X, Dong X, Cui M, Dong C, Yang Y. Pyrolysis mechanism of glucose and mannose: the formation of 5-hydroxymethyl furfural and furfural. J Energy Chem 2018;27:486–501.
- [33] Delbecq F, Khodadadi MR, Rodriguez Padron D, Varma R, Len C. Isosorbide: recent advances in catalytic production. Mol Catal 2020;482:110648.
- [34] Chen S, Wojcieszak R, Dumeignil F, Marceau E, Royer S. How catalysts and experimental conditions determine the selective hydroconversion of furfural and 5-hydroxymethylfurfural. Chem Rev 2018:118:11023—117.
- [35] Cheng Y-T, Huber GW. Chemistry of furan conversion into aromatics and olefins over HZSM-5: a model biomass conversion reaction. ACS Catal 2011;1: 611–28
- [36] Oh SC, Nguyendo T, He Y, Filie A, Wu YQ, Tran DT, Lee IC, Liu DX. External surface and pore mouth catalysis in hydrolysis of inulin over zeolites with different micropore topologies and mesoporosities. Catal Sci Technol 2017;7: 1153–66
- [37] Prasomsri T, To AT, Crossley S, Alvarez WE, Resasco DE. Catalytic conversion of anisole over HY and HZSM-5 zeolites in the presence of different hydrocarbon mixtures. Appl Catal B Environ 2011;106:204–11.
- [38] To AT, Resasco DE. Role of a phenolic pool in the conversion of m-cresol to aromatics over HY and HZSM-5 zeolites. Appl Catal Gen 2014;487:62–71.
- [39] Jae J, Tompsett GA, Foster AJ, Hammond KD, Auerbach SM, Lobo RF, Huber GW. Investigation into the shape selectivity of zeolite catalysts for biomass conversion. J Catal 2011;279:257–68.
- [40] Zheng A, Zhao Z, Chang S, Huang Z, Wu H, Wang X, He F, Li H. Effect of crystal size of ZSM-5 on the aromatic yield and selectivity from catalytic fast pyrolysis of biomass. J Mol Catal Chem 2014;383—384:23—30.
- [41] Parker DSN, Kaiser RI, Kostko O, Ahmed M. Selective formation of indene through the reaction of benzyl radicals with acetylene. ChemPhysChem 2015:16:2091—3.
- [42] Carlson TR, Cheng Y-T, Jae J, Huber GW. Production of green aromatics and olefins by catalytic fast pyrolysis of wood sawdust. Energy Environ Sci 2011;4: 145–61.
- [43] Martens JA, Verrelst WH, Mathys GM, Brown SH, Jacobs PA. Tailored catalytic propene trimerization over acidic zeolites with tubular pores. Angew Chem

- Int Ed 2005;44:5687-90.
- [44] Iisa K, Robichaud DJ, Watson MJ, ten Dam J, Dutta A, Mukarakate C, Kim S, Nimlos MR, Baldwin RM. Improving biomass pyrolysis economics by integrating vapor and liquid phase upgrading. Green Chem 2018;20:567–82.
- [45] Wei B, Jin L, Wang D, Shi H, Hu H. Catalytic upgrading of lignite pyrolysis volatiles over modified HY zeolites. Fuel 2020;259:116234.
- [46] Ma Z, Troussard E, van Bokhoven JA. Controlling the selectivity to chemicals from lignin via catalytic fast pyrolysis. Appl Catal Gen 2012;423–424:130–6.
- [47] Patel H, Hao N, Iisa K, French RJ, Orton KA, Mukarakate C, Ragauskas AJ, Nimlos MR. Detailed oil compositional analysis enables evaluation of impact of temperature and biomass-to-catalyst ratio on ex situ catalytic fast pyrolysis of pine vapors over ZSM-5. ACS Sustainable Chem Eng 2020:8:1762—73.
- [48] Guisnet M, Costa L, Ribeiro FR. Prevention of zeolite deactivation by coking. | Mol Catal Chem 2009;305:69–83.
- [49] Bhan A, Allian AD, Sunley GJ, Law DJ, Iglesia E. Specificity of sites within eightmembered ring zeolite channels for carbonylation of methyls to acetyls. J Am Chem Soc 2007;129:4919–24.
- [50] Huang X, Ludenhoff JM, Dirks M, Ouyang X, Boot MD, Hensen EJM. Selective production of biobased phenol from lignocellulose-derived alkylmethoxyphenols. ACS Catal 2018;8:11184–90.
- [51] Niziolek AM, Onel O, Guzman YA, Floudas CA. Biomass-Based production of benzene, toluene, and xylenes via methanol: process synthesis and deterministic global optimization. Energy Fuels 2016;30:4970–98.
- [52] Kumar R, Strezov V, Weldekidan H, He J, Singh S, Kan T, Dastjerdi B. Ligno-cellulose biomass pyrolysis for bio-oil production: a review of biomass pretreatment methods for production of drop-in fuels. Renew Sustain Energy Rev 2020;123:109763.
- [53] Cheng Y-T, Huber GW. Production of targeted aromatics by using Diels—Alder classes of reactions with furans and olefins over ZSM-5. Green Chem 2012;14: 3114—25.
- [54] Ibarra A, Hita I, Azkoiti MJ, Arandes JM, Bilbao J. Catalytic cracking of raw biooil under FCC unit conditions over different zeolite-based catalysts. J Ind Eng Chem 2019;78:372–82.
- [55] Zhang J, Sun G, Liu J, Evrendilek F, Buyukada M. Co-combustion of textile dyeing sludge with cattle manure: assessment of thermal behavior, gaseous products, and ash characteristics. J Clean Prod 2020;253:119950.
- [56] Atutxa A, Aguado R, Gayubo AG, Olazar M, Bilbao J. Kinetic description of the catalytic pyrolysis of biomass in a conical spouted bed reactor. Energy Fuels 2005:19:765-74.
- [57] Elordi G, Olazar M, Lopez G, Castano P, Bilbao J. Role of pore structure in the deactivation of zeolites (HZSM-5, H beta and HY) by coke in the pyrolysis of polyethylene in a conical spouted bed reactor. Appl Catal B Environ 2011;102: 224–31
- [58] Castano P, Elordi G, Olazar M, Aguayo AT, Pawelec B, Bilbao J. Insights into the coke deposited on HZSM-5, H beta and HY zeolites during the cracking of polyethylene. Appl Catal B Environ 2011;104:91–100.
- [59] Moljord K, Magnoux P, Guisnet M. Coking, aging and regeneration of zeolites: XVI. Influence of the composition of HY zeolites on the removal of coke through oxidative treatment. Appl Catal Gen 1995;121:245–59.